Letter

Universal power laws in two-dimensional diffusive search for randomly distributed targets

Rawan M. Nowier,* Nilaj Chakrabarty, and Peter Jung
Department of Physics and Astronomy and Quantitative Biology Institute, Ohio University, Athens, Ohio 45701, USA

(Received 22 April 2024; accepted 5 November 2024; published 8 January 2025)

We consider a two-dimensional diffusional search of randomly distributed targets characterized by their density and size. We derive analytical expressions for the binding rates averaged over ensembles of randomly distributed targets and initial positions of the searcher and test them through direct numerical simulations. These results suggest that the binding rates follow power laws over a wide range of target densities, with an exponent of about 1.1 for low densities and an exponent of 3/2 for larger densities. The transition between the two power laws depends on the size of the targets and searchers. We further predict linear dependence of the binding rate on the size of searchers and targets for small target densities.

DOI: 10.1103/PhysRevResearch.7.L012005

Introduction. Diffusive search of randomly distributed targets is common in the dynamics of disordered media (see references in [1]) and in biological systems [2,3]. Our interest in this topic is motivated by neurofilament transport along the neuronal axon. Neurofilaments are assembled in the cell body and transported by molecular motors along microtubule tracks in the axon. Long pauses in their movement may be caused by their detachment from their microtubule tracks and subsequent radial diffusional search for another microtubule, making microtubule density as well as microtubule and neurofilament sizes important determinants of the binding rate which controls neurofilament transport rate and axonal caliber [4]. Such dependence has important implications on axonal swelling and abnormal accumulations of neurofilaments observed in some neurodegenerative diseases [5,6]. Moreover, the diffusion of receptor proteins and other nanocargos within the two-dimensional cell membrane regulates key cellular processes such as signal transduction and endo- and exocytosis [7]. The rate at which these particles find and bind to their targets dictates the intracellular internalization process, and in turn the downstream signaling [8]. Our goal is to develop numerical and analytical insights into the average binding rates of searchers in a two-dimensional diffusive search with randomly distributed targets of a wide range of densities, and sizes of searchers and targets.

There is a large body of work on random searchers diffusing in a sea of stationary, randomly distributed targets of density n and binding to any one target where they get trapped [9–17]. For large times, the survival probability $P_s(t)$ of a searcher, i.e., the probability that the searcher has not been trapped after time t, has been shown to follow a stretched exponential $\exp(-k\,\lambda^{2/(d+2)}t^{d/(d+2)})$ [17,18]. Here d, assuming the values 1, 2, or 3, denotes the dimensionality of the problem and $\lambda = -\ln(1-c)$, where c is the fraction of lattice sites occupied by targets. The stretched exponential decay of the survival probability has been related to fluctuations of the local target density and associated large gaps between targets [16,17]. The behavior of the survival probability for small times has been discussed in [11,14,18]. For the more challenging case of $d = 2$, Gallos *et al.* [11] made specific predictions for the survival probability using an approximation by Henyey and Seshadri [19], which we will discuss below in view of our results.

Methods. Our analytical approximation to this problem is based on the statistical distribution of distances between N randomly distributed targets on a circular domain of area A. Equally dividing the total area over the N targets defines the Wigner-Seitz radius [20] $a = 1/\sqrt{\pi n}$, associated with the area per target, where n is the target density. The Wigner-Seitz radius a serves as a characteristic length scale in our system. If we choose one target as a reference point, we obtain the probability of finding no target within a circle of radius r as $P_1 = (1-\pi r^2/A)^{N-1} = [1-(r^2/a^2)(1/N)]^{N-1}$, which becomes $P_1 = \exp[-(r/a)^2]$ in the limit of large numbers N. Correspondingly, we can write the probability $\rho_1(r)dr$ of finding the nearest target within an infinitesimal radial shell $[r, r+dr]$ as the product of the probability $2\pi nrdr$ of finding a single target in the infinitesimal shell and $N-2$ targets outside the shell in the limit of large numbers N as

$$\rho_1(r) = \frac{2}{a}\frac{r}{a}\exp\left(-\frac{r^2}{a^2}\right). \tag{1}$$

This is a normalized probability distribution with an average nearest neighbor distance of $\langle r_1\rangle = 1/(2\sqrt{n})$ [21].

We can generalize this result to calculate the second and higher next-neighbor distance probabilities $\rho_M(r)dr$, which are the product of the probabilities of finding any $M-1$ of the N targets within the circle of radius r, and one of the $N-(M-1)$ remaining targets in the circular shell $[r, r+dr]$, and the remaining $N-M$ targets outside the circular shell. In

*Contact author: rn757120@ohio.edu

Published by the American Physical Society under the terms of the Creative Commons Attribution 4.0 International license. Further distribution of this work must maintain attribution to the author(s) and the published article's title, journal citation, and DOI.

the limit of large N we find

$$\rho_M(r) = \frac{2}{a}\frac{1}{(M-1)!}\left(\frac{r}{a}\right)^{2M-1}\exp\left(-\frac{r^2}{a^2}\right), \quad (2)$$

with the average Mth − order next-neighbor distance of

$$\langle r_M\rangle = a\,\frac{\Gamma(M+1/2)}{\Gamma(M)} = \frac{1}{\sqrt{\pi n}}\frac{\Gamma(M+1/2)}{\Gamma(M)}. \quad (3)$$

We tested these predictions numerically and found good agreement (see Fig. 1S in the Supplemental Material [22]). The results above are derived under the assumption that the targets are pointlike randomly distributed particles. However, as the target density or size increases, random positioning of the targets under the condition they do not overlap is not possible, deviating from the distribution of completely randomly placed targets. Hence the analytical estimates for the distance distributions described above become less reliable for large densities and larger target sizes.

To calculate the configuration averaged binding rate of a searcher starting at a random location within the circular domain, we decompose this rate as the sum over the contributions of binding the average nearest neighbor $\langle r_1\rangle$, the average next nearest neighbor $\langle r_2\rangle$, and so on. The mean first passage time for the center of a searcher of radius R_s to reach any point at the average distance $\langle r_M\rangle$ to the Mth nearest neighbor from its initial position is given by $T_{\mathrm{MFPT}} = \frac{\langle r_M\rangle^2}{4D}$, where D denotes the diffusion coefficient of the searcher [23]. Since there is only one Mth nearest target, the average rate at which the searcher finds this target becomes the inverse mean first passage time above multiplied by the probability of a searcher crossing a circle at distance $\langle r_M\rangle$ from its initial position at the section of the circumference where the actual nearest neighbor is located, i.e., $\frac{2(R_s+R_t)}{2\pi\langle r_M\rangle}$, or in summary,

$$\gamma_M = \frac{4D(R_s+R_t)}{\pi\langle r_M\rangle^3}. \quad (4)$$

This is the average rate at which a searcher finds the ensemble averaged Mth nearest target. For numerical tests of Eq. (4), see the Supplemental Material (Fig. 2S [22]). When searchers do not find and bind the nearest target, they will find a higher-order nearest neighbor target. Adding the average rate contributions through ensemble averaged neighbor distances of all orders M [see Eq. (3)], the rate of finding any target then becomes

$$\gamma = \sum_{M=1}^{\infty}\gamma_M = \frac{4}{\pi}D(R_s+R_t)\sum_{M=1}^{\infty}\frac{1}{\langle r_M\rangle^3} = 22.5\,D(R_s+R_t)n^{3/2}. \quad (5)$$

Most significantly, we predict that the overall binding rate is proportional to the target density n to the power $3/2$ with a linear dependence on the target and searcher size. This result is an approximation and is limited by the assumption that the searches that exceed the distance $\langle r_M\rangle$ will find a target at a larger distance $\langle r_{M'>M}\rangle$, or in other words, that the searchers do not successfully return to bind to targets at the smaller distance $\langle r_M\rangle$. The reason for this is twofold. First, even in the absence of targets, a diffusing particle in two dimensions or any other higher dimension executes radial spreading; i.e., the average distance from the initial point increases as $\langle r\rangle(t) = \sqrt{\pi Dt}$. Second, and more importantly, the presence of targets makes successful returns less likely because the searchers bind to other targets. For numerical estimates of the return probabilities and their target density dependencies, see Fig. 3S in the Supplemental Material [22]. Because of the limitations of the expected validity of Eq. (5), we use it only as guidance for our numerical studies below. We will test the validity of the power-law dependence on the target density and the linearity of the dependence on the sizes of the searcher and target and determine their limits.

We simulated the two-dimensional search problem on a circular domain of radius R_d with randomly placed N targets of radius R_t. We then place searchers of radius R_s (one at a time) at random locations on the circular domain so that they do not overlap with a target. The searchers perform two-dimensional diffusion according to

$$x(t+dt) = x(t) + \sqrt{2Ddt}G_x$$
$$y(t+dt) = y(t) + \sqrt{2Ddt}G_y, \quad (6)$$

where G_x and G_y are Gaussian random numbers with zero mean and unit variance, x and y are the Cartesian coordinates of a searcher, D is the diffusion coefficient of the searcher, and dt is the time step. We performed these simulations in effectively infinite-sized as well as finite-sized systems. For the infinite system, we scale the distances, system sizes, and searcher and target sizes, with the Wigner-Seitz radius $a = \frac{1}{\sqrt{\pi n}}$. We introduce the dimensionless variables $\bar{x} = \frac{x}{a}$, $\bar{y} = \frac{y}{a}$, and $\bar{t} = \frac{tD}{a^2}$, which results in a set of equations identical to Eq. (6) but with a unit diffusion coefficient. Accordingly, the radii of the targets, searchers, and the domain radius are also scaled by the Wigner-Seitz radius, i.e., $\overline{R_t} = \frac{R_t}{a}$, $\overline{R_s} = \frac{R_s}{a}$,and $\overline{R_d} = \frac{R_d}{a}$. The number of targets at a density n are given by $N = n\pi R_d^2 = \pi n a^2\overline{R_d}^2 = \overline{R_d}^2$. This means that for decreasing target densities, the Wigner-Seitz radius increases along with the actual system size R_d, while keeping the total number of targets and their density in scaled variables constant. This self-adjusting system size guarantees that the number of searches that find the boundaries before a target remains equally small for all densities. The searchers start in the center half of the circular domain so that the frequency at which they arrive at the boundary of the domain before they find a target is small. For the few cases (see Fig. 4S in the Supplemental Material [22] for a quantitative analysis) where this occurs, we terminate the search and do not record the time. The average binding rate has been obtained by taking the inverse of the average of 10 000 search times resulting from random configurations of the targets and randomly chosen initial positions of the searchers within one configuration of the targets, i.e., $\gamma = \frac{1}{\langle t\rangle}$. The statistical error σ_γ in the rates γ was calculated through $\sigma_\gamma = \frac{\sigma_t}{\langle t\rangle^2\sqrt{10\,000}}$, where σ_t is the standard deviation of the search times.

As for the finite-sized system, we use nonscaled variables in order to change the target density without changing the system size. We start the searcher randomly over the entire circular domain and reject the moves that result in searchers moving beyond the finite domain radius.

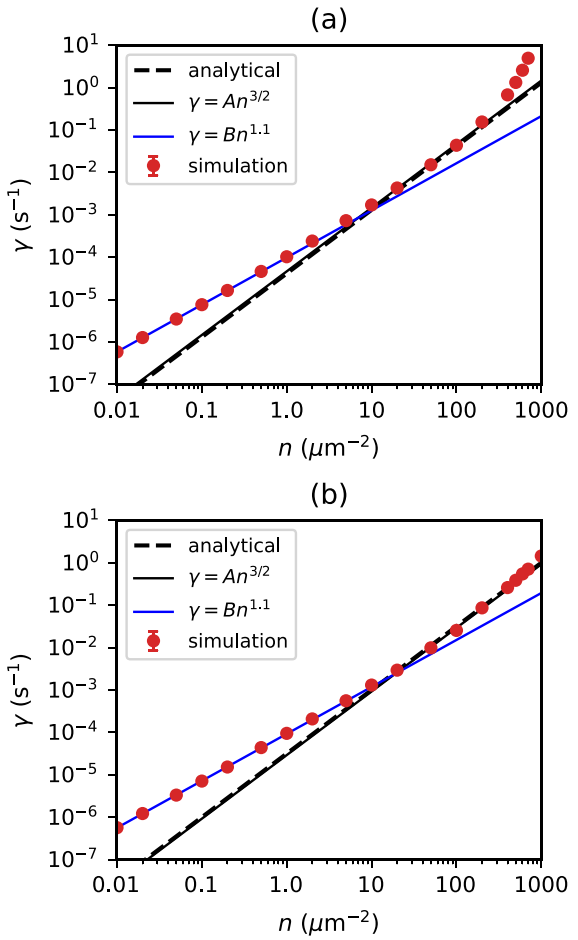

FIG. 1. Simulation results (solid circles) for the average binding rate γ as a function of target density n for searcher size of $R_s = 0.02\,\mu$m and target size of (a) $R_t = 0.0125\,\mu$m and (b) $R_t = 0.005\,\mu$m. The double logarithmic plots show the transition between two power-law dependencies. The high-density results were fitted to a power law that follows the equation $\gamma = An^{3/2}$ (black solid line), where for (a) $A = 4.62 \times 10^{-5}\,\mu$m^3/s and for (b) $A = 3.02 \times 10^{-5}\,\mu$m^3/s. The low-density results were fitted to a power-law regression of $\gamma = Bn^{\alpha}$ that resulted in an exponent of $\alpha = 1.1$ (blue line). The scaling factors are (a) $B = 9.75 \times 10^{-5}\,\mu$m^3/s and (b) $B = 9.27 \times 10^{-5}\,\mu$m^3/s. The dashed black line represents the analytical prediction in Eq. (5). Statistical error bars are smaller than the symbols.

Results. We first discuss the binding rates γ at which searchers bind targets as a function of their density n in infinite systems. Figure 1(a) shows the binding rate γ, on a double logarithmic plot for standard radii of the searchers $R_s = 0.02\,\mu$m and targets $R_t = 0.0125\,\mu$m. These sizes were chosen based on our application to axonal transport. The results in panel (b) were produced using smaller target radii of $R_t = 0.005\,\mu$m in order to test the effect of target size. For large densities, the simulations fit well the prediction in Eq. (5), i.e., $\gamma \propto n^{3/2}$ (black dashed line). The predicted prefactor of the rate in Eq. (5) is slightly different than for the regression (see solid black line). The prefactor reflects the distribution of the distances between the targets and a geometric factor [see Eq. (4)].

The double logarithmic plot indicates that the predicted power-law dependence on the target density in Eq. (5) is robust for target densities up to about 200 /μm^2 for standard sizes of searcher and targets. The deviations for larger target densities are caused by local confinement of the searcher. If the gaps are too small, the searcher is confined to a local search domain and will not be able to bind to targets further away, thereby increasing the average binding rates. To be more quantitative, we consider the density percolation threshold above which the searcher is confined at all initial positions. We estimated the percolation threshold computationally by diffusing particles in 1000 random configurations of targets starting in the center of the domains and rejecting moves that collide with targets. Above the percolation threshold of about 250 /μm^2 for standard-sized searchers and targets and about 2500 /μm^2 for target sizes of $R_t = 0.005\,\mu$m, no searcher reaches the domain boundaries. We see that the onset of deviations from the 3/2 power law coincides approximately with the respective percolation thresholds.

As for the smaller target densities, the double logarithmic plot reveals a transition to a different power-law dependence, i.e., $\gamma \propto n^{\alpha}$ with a power of $\alpha = 1.1$. This change of power may be interpreted as a transition from a local neighborhood search for larger target densities to a more global search at small target densities. The transition density, as determined by the intersection of the two regressions, is at approximately 10 /μm^2 for standard R_t and R_s sizes [panel (a)], and 25 /μm^2 for $R_t = 0.005\,\mu$m and $R_s = 0.02\,\mu$m [panel (b)]. For more combinations of target and searcher sizes, see Fig. 5S in the Supplemental Material [22].

Next, we discuss the effect of target and searcher sizes on the binding rates γ, testing the linear dependencies on the sizes as predicted in Eq. (5). In Fig. 2(a), we show the dependence of γ on the radius of the targets R_t for $n = 10$ /μm^2, $n = 30$ /μm^2, and $n = 50$ /μm^2 at a fixed value of the searcher size $R_s = 0.02\,\mu$m. The dashed lines represent linear regressions. For small target sizes at all densities, the rate follows a linear dependence as predicted in Eq. (5). As n increases, deviations occur at a decreasing target size R_t. The onset of deviations from the linear dependence is almost independent of the size of the searchers (see Fig. 6S [22]), indicating that the deviations may reflect the above-described nonrandomness in the distribution of the targets. In Fig. 2(b), we show the dependence of the rate γ on the size of the searcher R_s. The predicted linear dependence on the size of the searcher is valid in a larger range of searcher sizes than for the sizes of the targets shown in panel (a). In contrast to the theory in Eq. (5) where the sizes of the targets and searchers enter symmetrically, the actual dependence is not symmetric for larger target sizes because the distribution of the targets for finite target sizes depends on the target sizes.

We now discuss the effect of a finite system size on the results shown above. To determine the rates at a specific system size we used nonscaled variables and kept the target and searcher sizes constant at $R_t = 0.0125\,\mu$m and $R_s = 0.02\,\mu$m, respectively. When a search meets the system boundary before it finds a target, we reject any random move that would result in a movement beyond the system size. We find that the rates do not depend on the system size as small as at least $R_d = 0.5\,\mu$m (for details, see Fig. 7S [22]). At smaller domain

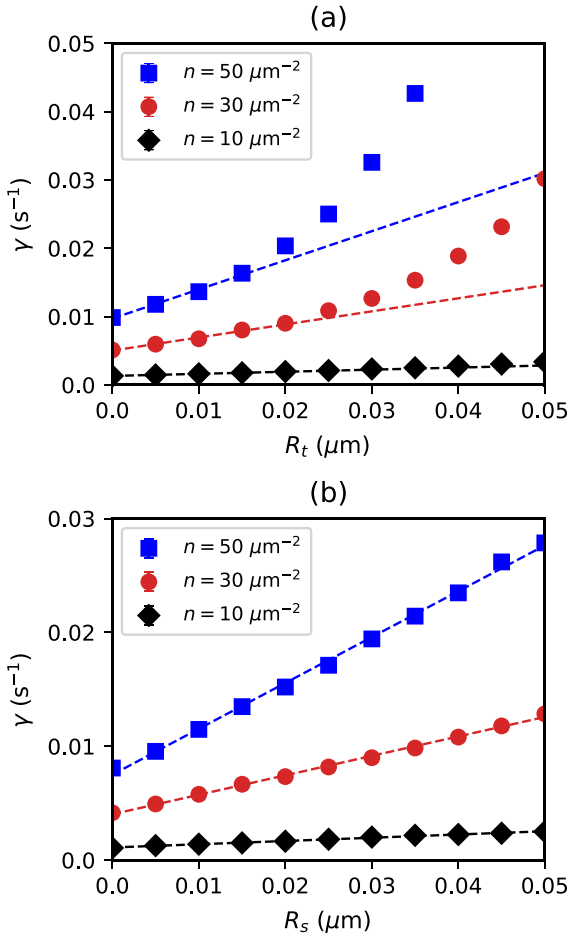

FIG. 2. Particle size dependence of the binding rate γ at target density $n = 10\,/\mu m^2$ (black diamonds), $30\,/\mu m^2$ (red circles), and $50\,/\mu m^2$ (blue squares). The dashed lines represent linear regressions. (a) Simulation results (symbols) for γ as a function of the size of the target R_t. (b) Simulation results (symbols) for γ as a function of the size of the searcher R_s. Statistical error bars are smaller than the symbols.

areas $A = \pi R_d^2$, a given density n cannot be represented well by $\frac{N}{A}$ because it is discrete, and we do not discuss this limit here. We tested and confirmed the consistency of the rates versus the system for target and searcher sizes between 0.005 and 0.05 μm (not shown). An explanation for the system size independence could be that a search outside the actual system size would be indistinguishable from a search within the bounds of the system because the micro search environments are the same.

Discussion. In this Letter we considered the binding rates of diffusive searchers for randomly distributed targets in a two-dimensional circular domain. Instead of diffusion on a lattice used in previous works in the literature, we consider continuous diffusion and study the dependence of the binding rates on target density, and sizes of targets and searchers. We found that the binding rates follow power-law dependencies on the density of targets with an exponent of 1.1 for small densities and an exponent of 3/2 for larger densities limited by confinement. The transition between the two power laws is influenced by the size of the targets and reflects a transition between a global and a local search (see Fig. 8S [22]). The reason the 3/2 scaling becomes invalid for smaller densities can be explained by the different distributions of the nearest neighbor distances for low and high densities. In the low-density regime, the distributions of nearest neighbor distances become very broad (see Fig. 9S [22]), exhibiting large fluctuations translating into large fluctuations in the distributions of search times such that the search time to the average distance as used in Eq. (4) no longer reflects the search process.

The fact that the binding rate increases with target density in a more than linear fashion has profound practical implications as it is more sensitive to changes thereof. For example, neurofilament transport operates within the 3/2 power-law regime, as supported by available morphometric data ([4] and references therein). The nonlinear relation makes the axon caliber, which must be matched to neuron function, more sensitive to changes in neurofilament kinetics [4]. According to the equation of continuity, at a constant flux of neurofilaments a decline in the average transport velocity v of neurofilaments leads to their accumulation in the axon, increasing the axonal cross-sectional area A, such that $A \propto \frac{1}{v}$. Given that v is proportional to the neurofilament binding rate γ to microtubules [24], which itself scales with the density of microtubules n as $\gamma \propto n^m$, the axonal area A becomes proportional to n^{-m}. If the microtubule density decreases, e.g., by a factor of 2, the axonal area then increases by a factor of 2.8 when $m = 3/2$ compared to a factor of 2.1 if for $m = 1.1$. Therefore, the caliber is more sensitive to changes in kinetics for the larger exponent of 3/2, and this increased sensitivity may contribute to accumulation of neurofilaments observed in neurodegenerative diseases [5,6].

Another pathway to derive the 3/2 power-law dependence of the binding rates is based on the Wigner-Seitz scaling described in the Methods section. The constant target density in scaled variables implies that the scaled binding times only depend on $\overline{R_t}$ and $\overline{R_s}$. Transforming this back into the original timescale, i.e., $t = \frac{a^2}{D}\bar{t}$, implies the scaling relation for the binding rate $\gamma \propto nf(R_t\sqrt{n},\ R_s\sqrt{n})$ with a scaling function f. The linear dependence of the binding rate on the sum of the sizes of targets and searchers, as predicted in Eq. (5), requires a linear scaling function f and a $n^{3/2}$ density dependence. In other words, the $n^{3/2}$ dependence of the binding rates is linked to a linear dependence on the target size.

In the literature on diffusive search problems, the survival probabilities of the searcher are often considered to characterize the search process. The binding rates discussed here are related to the survival probability and can be calculated from them. The probability density of binding times $\rho_b(t)$ corresponds to the survival probability $P_s(t)$ according to $\rho_b(t) = -\dot{P}_s(t)$, and hence for the average binding time we find

$$\langle t_b \rangle = \int_0^\infty \rho_b(t) t\,dt = -\int_0^\infty \dot{P}_s(t) t\,dt = \int_0^\infty P_s(t)\,dt, \quad (7)$$

and an average binding rate of $\gamma = 1/\langle t_b \rangle$. This calculation, however, requires the entire time course of the survival probability which is generally not known except in the limits of small and large times.

Using the asymptotic expression for the survival probability $P_s(t)$ (see Introduction) which is derived from a lattice-based model, the average survival rate is proportional to $-1/\ln(1-c)$, where c is the fraction of sites with targets. For a small fraction of targets, this results in a linear dependence, which is close to what we find for small densities of targets n, i.e., $\gamma \propto n^{1.1}$. However, the $3/2$ power-law dependence of the rates for larger target densities is not obtained from this asymptotic limit. The expression for the survival probability for small times, put forward by [11] [see Eq. (17) therein] in conjunction with Eq. (7), results in a rate $\gamma \propto n^{1/0.9}$, which is consistent with our numerical results for small target densities. The reason for the agreement is that their short-time behavior of the survival probability at small target densities is valid for large enough times that the integral in Eq. (7) becomes accurate (see [11] for a discussion of the validity of their short-time approximation).

Open questions for future research are how binding times behave in a three-dimensional (3D) diffusional search.

Acknowledgments. We thank the National Science Foundation for financial support through Grant No. IOS-1656765 and we thank Professor Horacio Castillo from Ohio University for discussion.

[1] S. Havlin and D. Ben-Avraham, Diffusion in disordered media, Adv. Phys. **36**, 695 (1987).
[2] A. I. Brown, L. M. Westrate, and E. F. Koslover, Impact of global structure on diffusive exploration of organelle networks, Sci. Rep. **10**, 1 (2020).
[3] C. Z. Scott, A. I. Brown, S. S. Mogre, L. M. Westrate, and E. F. Koslover, Diffusive search and trajectories on tubular networks: A propagator approach, Eur. Phys. J. E **44**, 80 (2021).
[4] R. M. Nowier, A. Friedman, A. Brown, and P. Jung, The role of neurofilament transport in the radial growth of myelinated axons, Mol. Biol. Cell **34**, ar58 (2023).
[5] K. J. De Vos, A. J. Grierson, S. Ackerley, and C. C. J. Miller, Role of axonal transport in neurodegenerative diseases, Annu. Rev. Neurosci. **31**, 151 (2008).
[6] S. Millecamps and J.-P. Julien, Axonal transport deficits and neurodegenerative diseases, Nat. Rev. Neurosci. **14**, 161 (2013).
[7] E. D. Gundelfinger, M. M. Kessels, and B. Qualmann, Temporal and spatial coordination of exocytosis and endocytosis, Nat. Rev. Mol. Cell Biol. **4**, 127 (2003).
[8] L. Xiao, L. Wei, C. Liu, Y. He, and E. S. Yeung, Unsynchronized translational and rotational diffusion of nanocargo on a living cell membrane, Angew. Chem., Int. Ed. **51**, 4181 (2012).
[9] H. B. Rosenstock, Random walks on lattices with traps, J. Math. Phys. **11**, 487 (1970).
[10] J. K. Anlauf, Asymptotically exact solution of the one-dimensional trapping problem, Phys. Rev. Lett. **52**, 1845 (1984).
[11] L. K. Gallos, P. Argyrakis, and K. W. Kehr, Trapping and survival probability in two dimensions, Phys. Rev. E **63**, 021104 (2001).
[12] R. F. Kayser and J. B. Hubbard, Diffusion in a medium with a random distribution of static traps, Phys. Rev. Lett. **51**, 79 (1983).
[13] J. W. Haus and K. W. Kehr, Diffusion in regular and disordered lattices, Phys. Rep. **150**, 263 (1987).
[14] G. T. Barkema, P. Biswas, and H. van Beijeren, Diffusion with random distribution of static traps, Phys. Rev. Lett. **87**, 170601 (2001).
[15] M. D. Donsker and S. R. S. Varadhan, Asymptotics for the Wiener sausage, Commun. Pure Appl. Math. **28**, 525 (1975).
[16] B. Ya. Balagurov and V. G. Vaks, Random walks of a particle on lattices with traps, Zh. Eksp. Teor. Fiz. **65**, 1939 (1973).
[17] P. Grassberger and I. Procaccia, The long time properties of diffusion in a medium with static traps, J. Chem. Phys. **77**, 6281 (1982).
[18] J. Schotland, Short-time behavior of diffusion with random traps, J. Chem. Phys. **88**, 907 (1988).
[19] F. S. Henyey and V. Seshadri, On the number of distinct sites visited in 2D lattices, J. Chem. Phys. **76**, 5530 (1982).
[20] N. W. Ashcroft and N. D. Mermin, *Solid State Physics*, 1st ed. (Cengage Learning, New York, 1976).
[21] P. Hertz, Über den gegenseitigen durchschnittlichen abstand von punkten, die mit bekannter mittlerer dichte im raume angeordnet sind, Math. Ann. **67**, 387 (1909).
[22] See Supplemental Material at http://link.aps.org/supplemental/10.1103/PhysRevResearch.7.L012005 for additional figures and detailed analyses.
[23] S. Redner, *A Guide to First-Passage Processes*, illustrated ed. (Cambridge University Press, Cambridge, UK, 2001).
[24] P. Jung and A. Brown, Modeling the slowing of neurofilament transport along the mouse sciatic nerve, Phys. Biol. **6**, 046002 (2009).